Chapter 6

Impedance-Based Health Monitoring with Artificial Neural Networks

6.1 Introduction

One of the important aspects of structural health monitoring is that the technique provides information on the life expectancy of structures, as well as detects and locates structural damage. In general, this requires knowledge of the model of structures in great detail, which is not always possible. In addition, dynamic systems usually present non-linear characteristics, imposing a difficulty on detecting and identifying structural damage for model-based damage detection techniques.

Artificial Neural Networks (ANN) have recently emerged as a promising tool for monitoring and fault classifications of systems and structures. ANN is well suited for solving inverse variational problem in the context of monitoring and fault detection because of their pattern recognition and interpolation capabilities (Lopes *et al*., 1997). ANN may also successfully approach and classify the problems associated with non-linearities, provided they are well represented by input patterns, and this approach can avoid the complexity introduced by conventional computational methods. Furthermore, the learning capabilities of ANN are well suited to process a large number of distributed sensors, which is ideal for smart structures.

This chapter describes a structural health monitoring technique, which combines these ANN features with the impedance-based method. Due to the high frequency range, the impedance-based technique is very sensitive to minor changes in the near field of piezoelectric sensor. However, due to the difficulties in developing an analytical model at such high frequency ranges, this technique can not correlate a change in electrical impedance with a specific

change in structural properties, hence it only provides limited information on the nature of damage. Therefore, a method, integrating the impedance-based technique with neural network features, has been developed to establish a robust and quantitative health monitoring system.

6.2 Principle of Artificial Neural Networks

Artificial Neural Network (ANN) is made by a number of processing elements that are connected to form layers of neurons. Each neuron is a simple mathematical processing unit that, when combined with other neurons, produces complex structures that can be trained to recognize defined patterns. The topologies and size of the networks depend on the specific application, and the definition of an optimal choice is also case dependent (Worden and Tomlinson, 1992). Figure 6.1 shows the pattern architecture with one hidden layer.

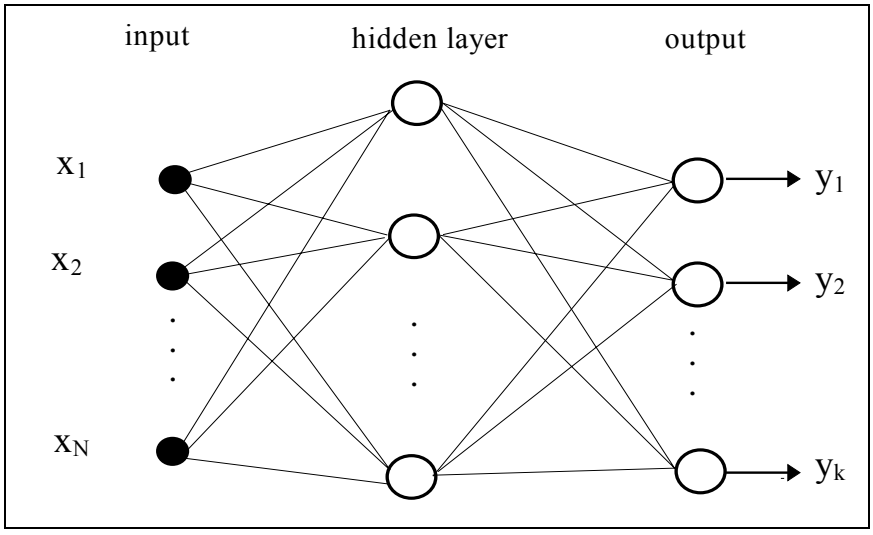

Figure 6.1 Architecture of the neural network with one hidden layer

The input to the ANN are the variables, (x_1, x_2, ...x_N), which are weighted by $w^h_{j,i}$, bias b^h_j , and the output results, (y_1, y_2, ...y_k), feed the hidden layer. The output of the j^{th}-hidden unit can be described by:

$$y^h_j = F_1\left(b^h_j + \sum_{i=1}^{N} W^h_{j,i} . x_i \right) \tag{6.1}$$

where the superscript (h) means that the quantities pertain to the hidden layer and $F_1(\bullet)$ is a sigmoid nonlinear function. The output of the ANN is biased and weighted by sum of the hidden layer outputs:

$$y_l = F_2\left(b^o_l + \sum_{j=1}^{H} W^o_{j,i} . y^h_j \right) \qquad l = 1, 2, \ \ldots , k \tag{6.2}$$

the superscript (o) refers to the output unit. H is the number of units in the hidden layer and $F_2(\bullet)$ is a linear activation transfer function. The ANN is trained starting with a random set of weights, and biases and the outputs are calculated for every input set. The error E is then computed from the output layer backwards, which has historically been called the backpropagated error. This learning procedure is called backpropagation algorithm. Several publications (Lippmann, 1987), have presented details of this algorithm. The error E is given by,

$$E = \text{sumsqr}(\{T\} - \{y\}) \tag{6.3}$$

where *sumsqr* is the sum of square of the elements, and T is the desired output. The error E is formulated as a function of the weights and biases, and the minimization is performed by means of the usual descent algorithm. The error E is denoted by $\{\alpha_j\}$, where the index j taking on as many values as there are weights and biases. When the parameter α_j changes by $\delta\alpha_j$, the error E changes by

$$\delta E = \frac{\partial}{\partial \alpha_j}(E)\,\delta\alpha_j \tag{6.4}$$

where $\frac{\delta}{\delta\alpha_j}(E)$ represents using the current values of the parameter. To ensure that changes in α_j results in a decrease in E, select,

$$\delta\alpha_j = -\eta\frac{\partial}{\partial\alpha_j}(E) \tag{6.5}$$

where η is a positive constant. The parameter η determines how large a step is made in the direction of the steepest descent and therefore how quickly the optimum parameters are obtained. For this reason, η is called the learning coefficient.

The training of the network uses a set of inputs for which a specified outputs is already known. The training process finishes when the error ***E*** is smaller than a desired value or it reaches a maximum specified number of iterations. In the later case, the training set is considered unsatisfactory. The error E considered herein is the sum of the squared error between the output value provided by the trained network and the value obtained for a specific input. The output can be a combination of zeros and ones, depending on each fault location and on the conditions of operations.

6.3 Damage Identification Scheme

The proposed damage identification scheme consists of two steps, as depicted in Figure 6.2. In the first step, the impedance-based method is used to detect and locate structural damage and provides a damage indication in a green/red light form. If it gives a red signal, the neural networks, which are trained for each specific damage, are used to estimate the severity of damage, as a second step.

The electrical impedance curves measured at very high frequency range show extreme sensitivity to changes in the structure. By this extreme sensitivity, it has been experienced that correlating impedance curve variations to each specific damage is very difficult in order to train the neural networks. Therefore, after the acquisition of the electrical impedance, the signals are need to be pre-processed and to be normalized in order to represent all conditions to be monitored and to be used as input patterns for the ANN.

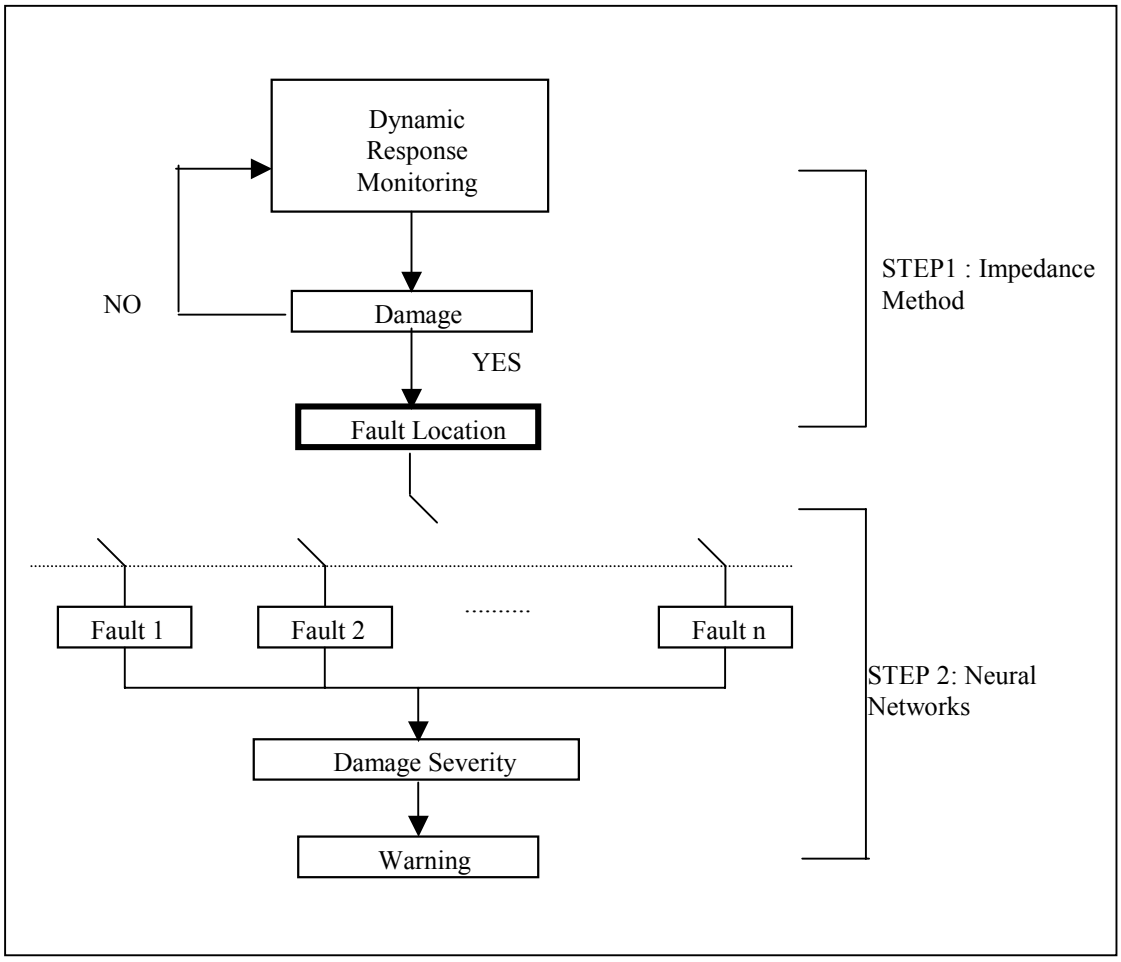

Figure 6.2 Diagram of the damage detection scheme

The pre-processed values utilized to train the ANN were:

i) the area between the undamaged and the damaged impedance curves,

ii) the root means square (rms.) of each curve,

iii) rms. difference between the undamaged and damaged curves,

iv) the correlation coefficient between the undamaged and damaged curves.

These values were obtained for both real and imaginary part of the impedance. Therefore, the input vector and input layer of the ANN consists of eight elements. Theoretically, one can use any data as inputs for ANN, however, the accuracy and generalization capacity of neural networks is strongly dependent on the choice of input patterns. The backpropagation algorithm was applied for the training processes.

The damage identification scheme developed herein is based on the sensitivity of electrical impedance to the presence of damage. By incorporating the use of neural networks, this approach is expected to be able to provide quantitative information on the nature of damage.

6.4 Simulation Results

Before experimental investigations were performed, a simulation example is used to test and to validate the method presented above, especially for the normalized data sets for the ANN inputs. The test structure is a seven finite element, free-free bar, which undergoes a longitudinal vibration. Simulated data are generated by wave finite element model. Damage, in the form of an increase in wavenumber, was introduced in each element. The wavenumber was increased up to 30%, in steps of 5%. The 5% change in wavenumber is equivalent to decrease in Young's Modulus by 10%, which induces a reduction of stiffness. The typical results, damage in 1^{st} and 4^{th} element, are shown in Figure 6.3.

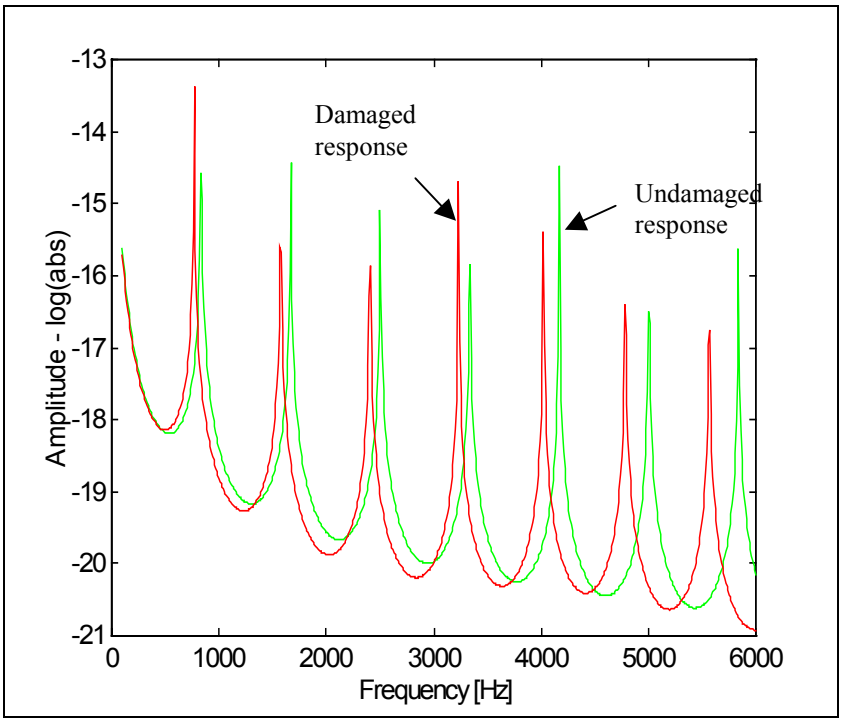

(a) element 1

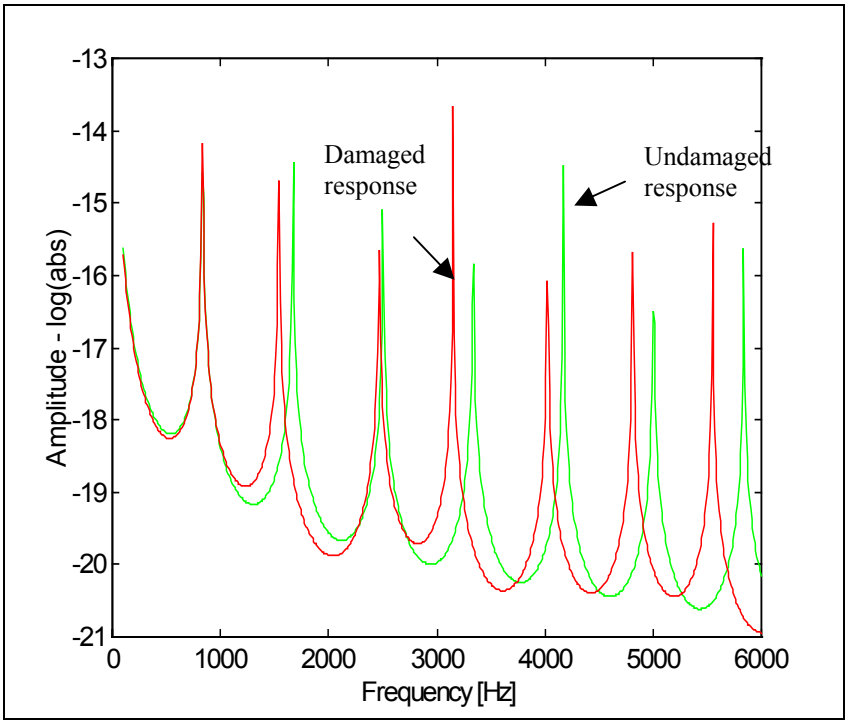

(b) element 4

Figure 6.3 Undamaged and damage responses (30 % increase in wave number)

As can be seen in Figure 6.3, when the element 1 is damaged the variation of the first resonant frequency is significant, compared to that the element 4 is damaged. If the element 4 is damaged, no variation in the first resonant frequency was observed, whereas the third and fifth resonant frequency shows relatively large variations. The ratio of the frequency changes in each mode is therefore only a function of the damage location (Cawley and Adams, 1979). Hence, the normalization scheme based on the sensitivity of the resonant frequency to the damage was applied to locate the damaged element in this structure.

The normalized value used to locate damage was obtained by the following equation:

$$dat1_i^j = \frac{\left(\omega_{und}^j - \omega_{di}^j\right)}{\omega_{und}^j} \Bigg/ \max\left\{\frac{\omega_{und}^j - \omega_{di}^j}{\omega_{und}^j}\right\}_i \qquad \text{with } \begin{matrix} j = 1,\ldots,7 \\ i = 1,\ldots,6 \end{matrix} \tag{6.6}$$

where ω_{und}^j is the jth natural frequency of the undamaged structure, ω_{di}^j is the jth natural frequency for the structure with fault *i* (wavenumber reduction of 5%, 10%, …, 30%).

Another normalization procedure was performed based on the variations of the natural frequencies due the damage severity.

$$dat2_i^j = 100\,\frac{\left(\omega_{und}^j - \omega_{di}^j\right)}{\omega_{und}^j} \qquad \text{with } \begin{matrix} j = 1,\ldots,7 \\ i = 1,\ldots,6 \end{matrix} \tag{5.7}$$

The first normalized values (*dat1*) are used to locate structural damage, whereas the second values (*dat2*) are used for estimate the severity of damage.

Two network configurations were developed to test the generalization capacity of this methodology: the first one with a single hidden layer and 10 neurons, and the second one with two hidden layers and 5 neurons in each layer. After the successful completion of the training procedure, this network was used to test the damage identification in a free-fee bar. Simulated data were generated to represent eight different damage situations, as shown in Table 5.1. Only one point of measurement was utilized to detect and locate the damage in this example.

	Test Value		**Identified**		
Fault Number	**Damaged element**	**Damage (%)**	**Damage Location**	**Damage 1 layer**	**Severity 2 layers**
Test 1	**1**	**23**	1	24.6	26.2
Test 2	**2**	**27**	2	25.1	25.0
Test 3	**4**	**3**	4	5.0	2.2
Test 4	**3**	**8**	3	9.5	6.7
Test 5	**4**	**19**	4	21.6	20.4
Test 6	**1**	**11**	1	11.5	9.06
Test 7	**3**	**21**	3	21.6	21.4
Test 8	**2**	**17**	2	19.2	17.7

Table 6.1 Results for the NN with one and two hidden layers

The second column of the table 5.1 shows the elements where the damage was introduced and the third column indicates the amount of reduction in the wavenumber. The fourth column in this table shows the results of the locating scheme of this methodology. It can be seen that the location of damage was correctly identified for every tested case. The fifth and sixth columns show the results obtained for the two network configurations. As can be seen, the severity of the damage elements was identified with reasonably small errors. Note that the amounts of reduction in wavenumbers were chosen between those values used for the training process. By this study, the use of normalized data sets for the ANN inputs was verified and this technique is extended to the experimental verification.

6.5 Proof-of-Concept Applications

6.5.1 A quarter scale bridge section

A quarter scale model of a steel truss bridge joint has been again investigated. The objective of this experiment was to test the ability of this proposed technique to detect, locate and characterize damage on this structure. A model of a steel bridge joint is shown in Figure 6.4. The bridge model consists of steel angles, channels, plates, and joints with over 200 bolts. The size of this structure is 1.8 m tall and has a mass of over 250 kg. Four PZT sensor/actuators (7 x 7 x 0.19 mm) are bonded on the critical sections to actively monitor the conditions of this typical high-strength civil structure. The combined approach, consisting of the impedance-based method and neural networks, has been used to interrogate this structure.

Damage was introduced by completely loosening bolts over several locations on the structure. The HP4194 electrical impedance analyzer was used for measurements of the PZT's electric impedances. The junctions connected with the bolts are considered to be critical to maintain the integrity of entire structures hence, they need to be continuously monitored. No assumption on the location or extent of damage was made, as in the practical health monitoring problems.

The training processes of the ANN were realized by considering the impedance measurements for both undamaged and damaged situations. The damages were induced at the location of position 1 (near PZT1), position 2 (near PZT2), position 3 (near PZT3), and position 4 (near PZT4), as shown in Figure 6.4.

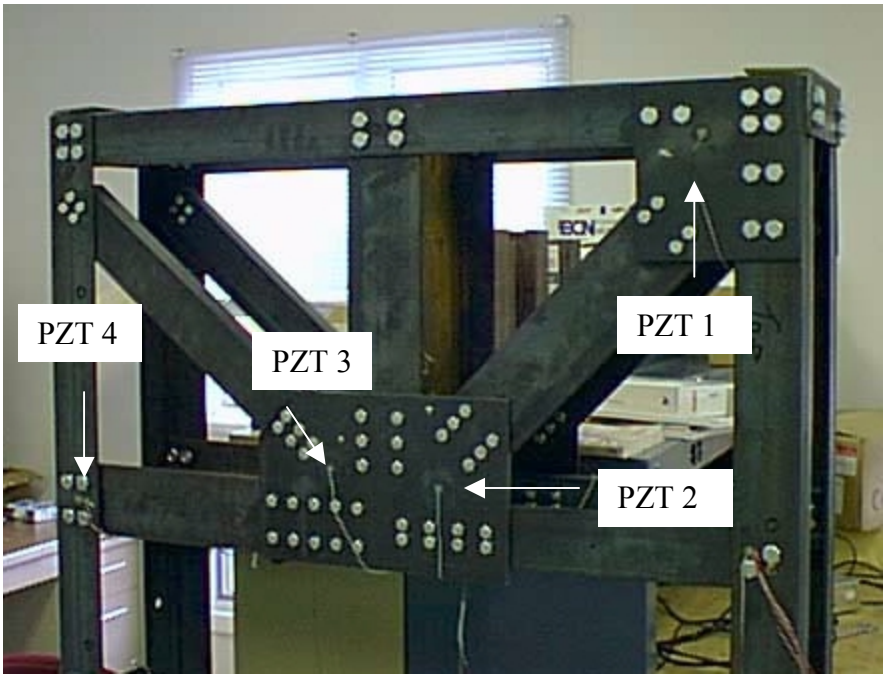

Figure 6.4 A ¼ scale steel bridge section

The multiple sets of measurements (for undamaged and damaged situations for all locations) were utilized to train the ANN. A sweep frequency range from 21 to 23 kHz was selected. Note that this frequency range is slightly lower than that of used in impedance-based method. This is because of the extreme sensitivity of each PZT sensor/actuator. Higher than 30 kHz ranges, repeatable undamaged impedance measurements (after inducing the damage) were very difficult to be obtained.

Each trained net monitors the damage only occurred in the vicinity of PZT sensors. Therefore, in this example, a total of four trained neural nets have been used to interrogate this structure. The training processes were completed before the experiments of impedance-based technique have been conducted. After successfully identifying the location of damage as detailed in chapter 3, a technique based on the use of neural networks has been used to estimate the severity of damage.

With the PZT 2 (position 2), the neural network was trained for the following specific damage situations:

- Undamaged - all six bolts tightened
- Damage 1 (D1) - loosening two bolts
- Damage 2 (D2) - loosening four bolts
- Damage 3 (D3) - loosening six bolts

Table 5.2 shows the experimental results obtained when damages were applied in the position 2. The ANN is trained to map the training data to the corresponding damage levels. The output range of the ANN for this step is from 0 to 3, which corresponds to undamaged situation, Damage 1, Damage 2, and Damage 3, respectively.

Damage Situation	D 1	D 2	D 3
ANN output	1.342	2.299	2.991

Table 6.2 Damage identified in the position 2

For the PZT 4, the following four different situations were considered.

- Undamaged - all bolts are tightened.
- Damage 1 – loosening bolts connecting upper channel
- Damage 2 – loosening bolts connecting lower-right channel
- Damage 3 – loosening bolts connecting diagonal channel

Table 5.3 shows the experimental results obtained when damages were applied in the position 4. The output range of the ANN for this step is from 0 to 3, which corresponds to undamaged situation, Damage 1, Damage 2, and Damage 3 respectively. As can be seen, this method is able to identify the severity of the damage with reasonable accuracy. The number of the loosening bolt, which can be correlated to the integrity of the entire structure, could be estimated. In summary, without prior knowledge of the model of structures, this methodology is able to monitor minor changes in structural integrity and to provide the nature of damage even in its early stage.

Damage Situation	D 1	D 2	D 3
ANN output	1.027	1.878	3.415

Table 6.3 Damage identified in the position 4

6.5.2 Analysis of a Space Truss Structure

Figure 6.5 shows a Brussels space bay truss structure consisting of pipe members and spherical Delrin balls. Each of the pipe members has a threaded connector at both ends, connected to a Delrin ball. Eight PZT patches (7 x 7 x 0.19 mm) are bonded to balls, labeled from A to H. Damage was simulated by loosening the connector thread. A sweep frequency range from 90 to 105 kHz was selected after several tests to find a high sensitive frequency range with good dynamic response. With the impedance-based approach, all the induced damages were clearly identified. The results of utilizing impedance-based technique are not shown in this chapter and a comprehensive report utilizing impedance-based technique to interrogate this structure can be found in the literature (Raju, 1998).

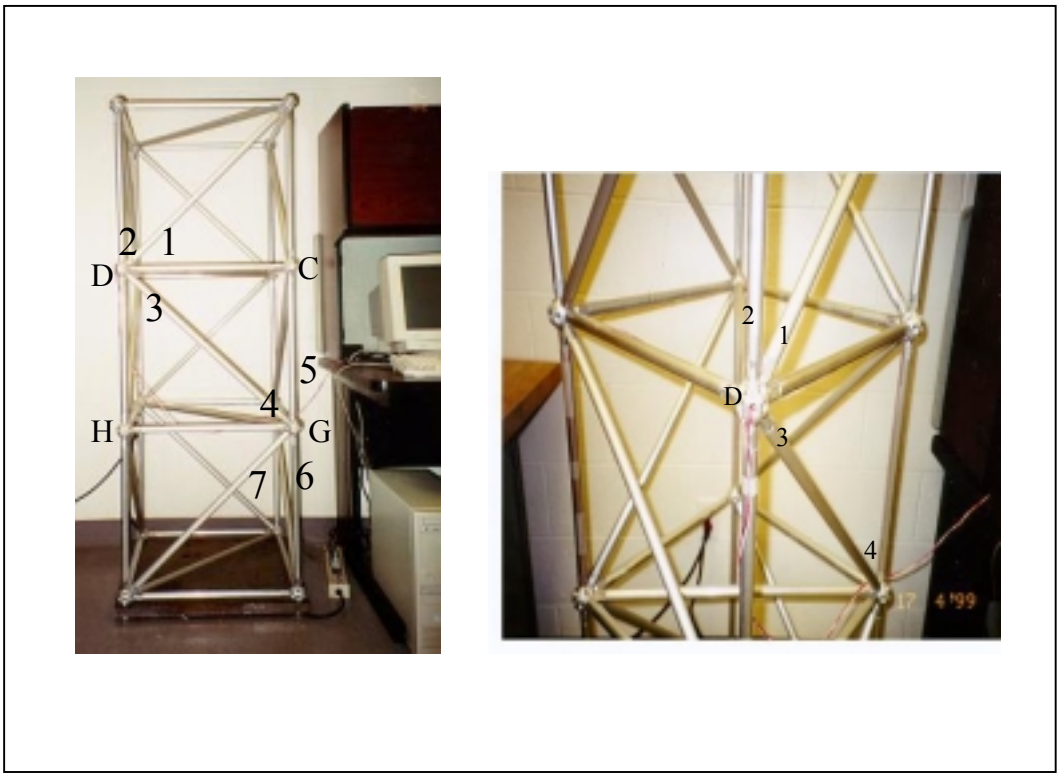

Figure 6.5 A space-bay structure with PZT bonded on balls

The training process of the ANN was performed by considering the impedance measurements for both undamaged and damaged conditions. For PZT D and G, following conditions were considered on this structure:

- Damage 1: Loosening element 1
- Damage 2: Loosening element 2
- Damage 3: Loosening element 3
- Damage 4. Loosening element 4
- Damage 5: Loosening element 5
- Damage 6. Loosening element 6
- Damage 7: Loosening element 7

Figures 6.6 shows real impedance measurements for the training process, obtained from PZT bonded on ball D. When damage 1, 2 and 3 were induced, which is very close to this sensor, significant variations in impedance signatures were observed. However, in the case of damage 4, 5, 6, and 7, only slight changes were observed since damages were induced far from the sensor.

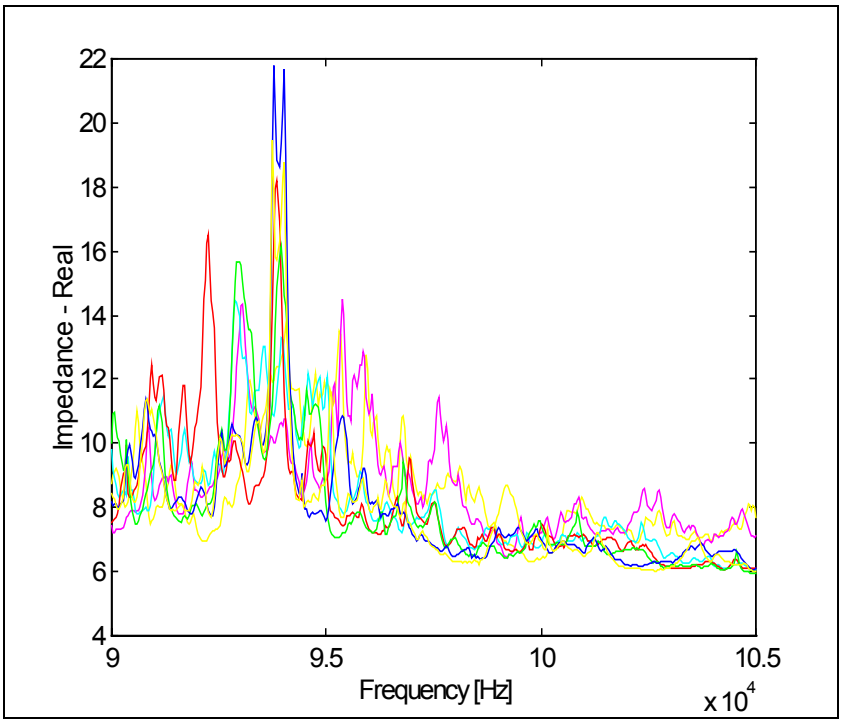

(a) Undamaged and damaged 1 to 3:

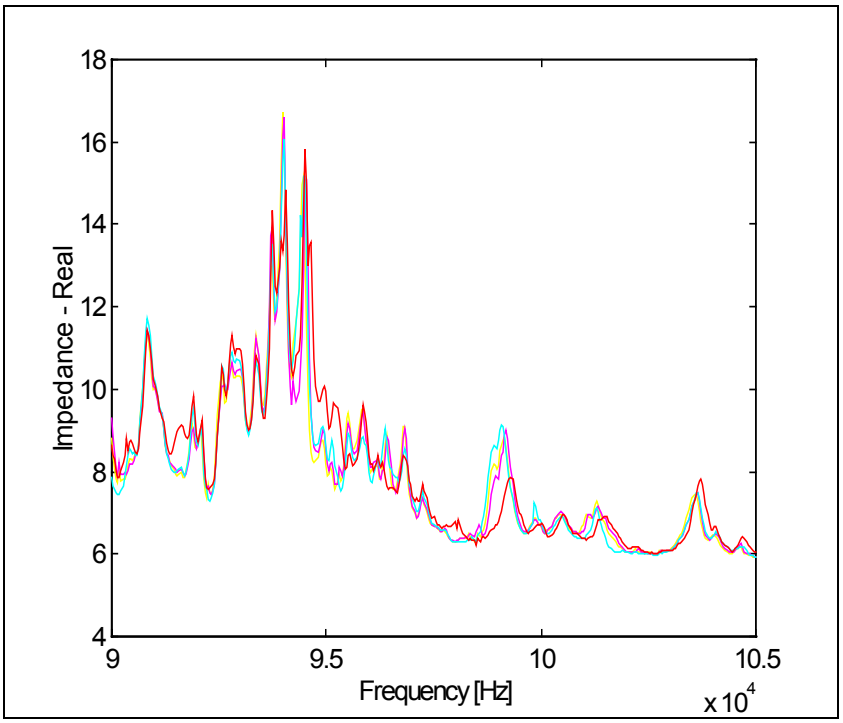

(b) Undamaged and damaged 4 to 6

Figure 6.6 Impedance measurements of PZT D

After the training processes were completed, all joints were tightened in order to return the structure to the initial condition. Several damages were introduced in this structure, and the trained neural networks were utilized to estimate the nature of damage. The following conditions were imposed to test the general capacity of ANN;

- Test 1. Loosening element 1
- Test 2. Loosening element 2
- Test 3. Loosening element 3
- Test 4. Loosening element 5
- Test 5. Loosening elements 1 and 7
- Test 6. Loosening elements 2 and 4
- Test 7. Loosening elements 2 and 5
- Test 8. Loosening elements 3 and 7

The tests 1 through 4 are correctly identified as expected, since the measured impedance curves of these conditions are almost identical to those utilized to train the neural networks. However, it is worth to point out that the test 5, 6, 7, and 8 are not included in the training data. Figure 6.7 and Figure 6.8 show the results of tests 7 and 8, obtained by the use of neural networks for PZT bonded on balls D and G, respectively. For PZT D (ball D), the net output values 0, 1, 2, and 3, correspond to undamaged, damage in element 1, damage in element 2, and damage in element 3, respectively. For PZT G (ball G), the net output values 0, 1, 2, 3, and 4 correspond to undamaged structure, damage in element 4, damage in element 5, damage in element 6, and damage in element 7, respectively. The results are normalized with the maximum value set to unity.

The damage of simultaneously loosening element 2 and element 5 (test 7) was identified as damage 2 (loosening of element 2) when analyzed by PZT D (figure 10a), and was identified as damage 5 (loosening of element 5) by PZT G (figure 10b). Figure 11a and 11b show the results for test 8. In these figures, the net output from PZT D identifies the damage in element 3, and the net output from PZT G identifies the damage in element 7 (output 4).

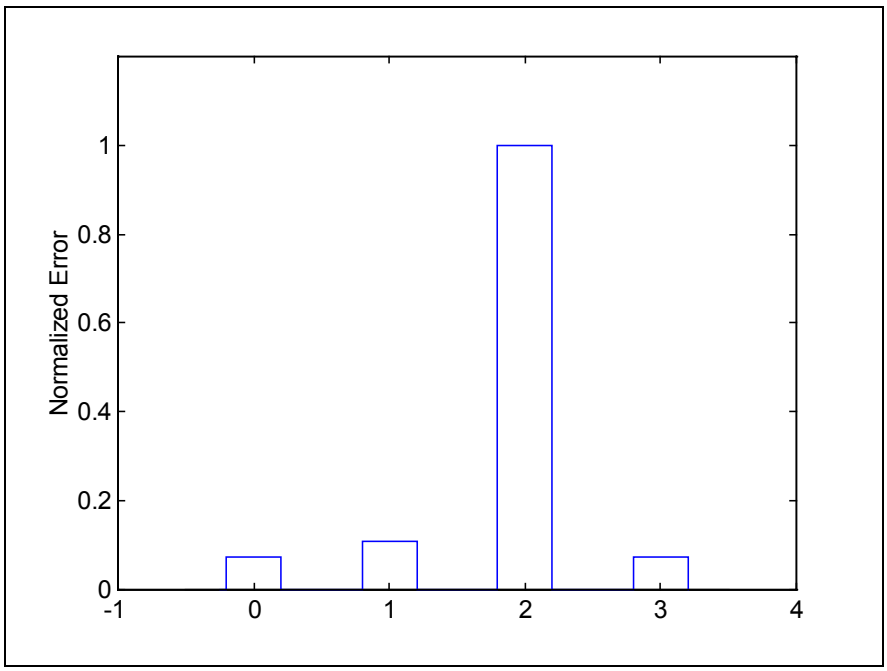

(a) PZT D

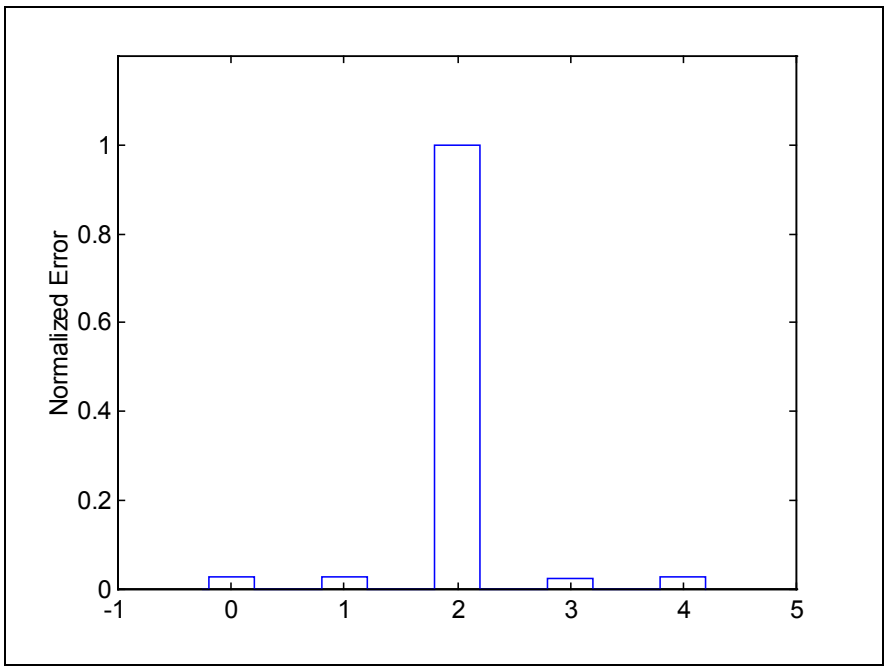

(b) PZT G

Figure 6.7 Results obtained by analyzing signals of Test 7

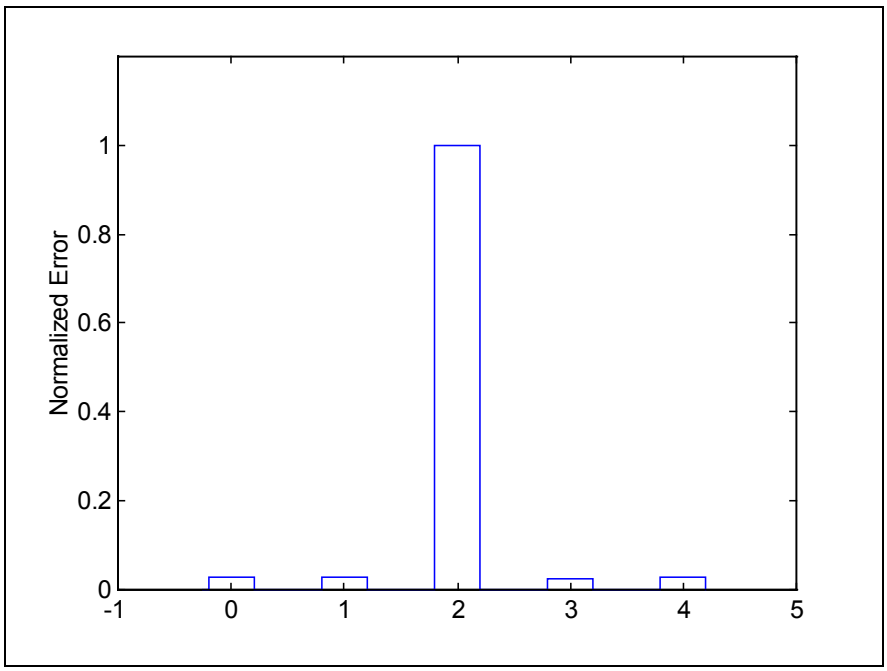

(a) PZT D

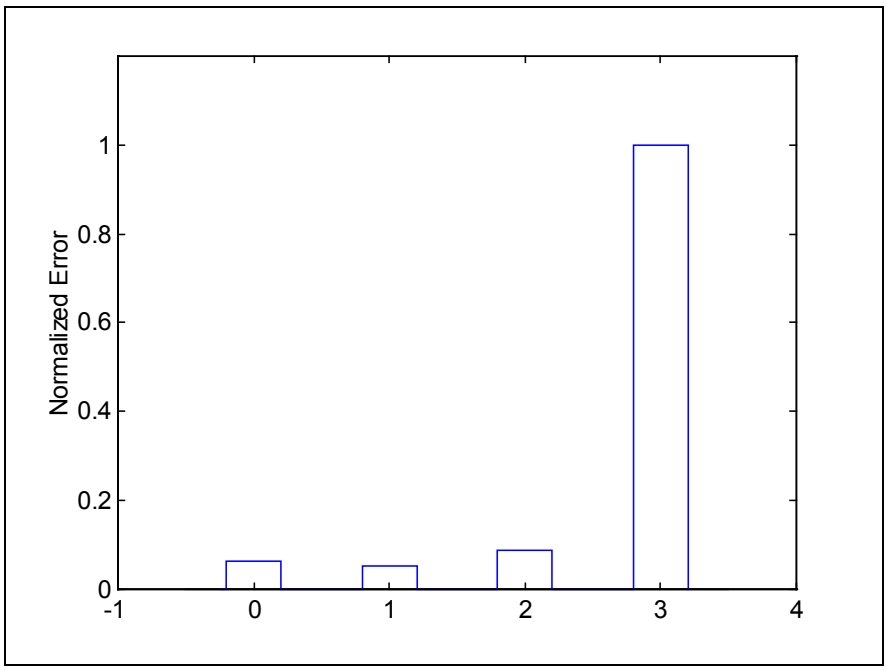

(b) PZT G

Figure 6.8 Results obtained by analyzing signals of Test 8

In the neural network based damage detection techniques, it is almost an impossible task to train the neural networks for all possible combination of multiple damages in different areas, if global frequency response functions are utilized to identify structural damage. However, as illustrated in this example, this method is able to monitor multiple damages at different locations, which were not contained in the training data. This is due to the high frequency range employed in this method. The high frequency structural excitation limits sensing area of each PZT sensors and helps to isolate the effect of damage on the signature from other far field changes. Thus, the signals from each PZT sensor can be analyzed separately and the amount of data that is needed for training processes can be drastically reduced.

5.6 Summary

This chapter presents a non-model based technique to detect, locate, and characterize structural damage by combining the impedance-based structural health monitoring technique with an artificial neural network. In order to quantitatively assess the state of structures, multiple sets of artificial neural networks, which utilize measured electrical impedance signals for input patterns, were developed. By employing high frequency ranges and by incorporating neural network features, this technique is able to detect the damage in its early stage and to estimate the nature of damage without prior knowledge of the model of structures. This technique would be more useful in identifying and tracking small defects, in the sense that damage is local phenomena and a high frequency effect. Experimental data sets were used to train the neural network. Thus, this technique is well suited for structures, where a prior analytical model is unknown and the excitation force is not available, Hence, the methods that utilize FRF are not applicable. Finally, the experimental examples, investigations on a massive quarter scale model of a steel bridge section and a space truss structure, were presented in order to verify the performance of this proposed methodology.